Sero-catalytic and spatial modeling of dengue virus force of infection in Timor-Leste

Paul Arkell[1,2,*$], Filipe de Neri Machado[3,4,*], Anna Vicco[5,*], Victoria M Cox[5,*], Maria Y Tanesi[1], Deolindo Ximenes[1], Wes Hinsley[5], Frederico Bosco[3,4], Nelia Gomes[1], Tessa Oakley[1], Vanessa Solano[6], Sarah L Sheridan[7], Michael David[8,9], Salvador Amaral[1], Luzia Freitas[5,10], Anthony DK Draper[1,11,12], Nevio Sarmento[1], Endang Soares da Silva[13], Lucsendar Alves[1], Neil Ferguson[5], Christl A Donnelly[14, 15], Jennifer Yan[1,+], Joshua R Francis[1,+], Ilaria Dorigatti[5,+], Nelson Martins[1 +]

1. Global and Tropical Health Division, Menzies School of Health Research, Charles Darwin University, Dili, Timor-Leste
2. Department of Infectious Diseases, Faculty of Medicine, Imperial College London, UK
3. Instituto Nacional de Saude Publica de Timor-Leste, Timor-Leste Ministry of Health, Dili, Timor-Leste
4. Departmanto Vigilancia no Epidemiojia, Timor-Leste Ministry of Health, Dili, Timor-Leste.
5. MRC Centre for Global Infectious Disease Analysis, Department of Infectious Disease Epidemiology, School of Public Health, Imperial College London, UK
6. Research Institute for the Environment and Livelihoods, Charles Darwin University, Darwin, Australia
7. National Centre for Immunisation Research and Surveillance (NCIRS), Westmead, NSW, Australia
8. Daffodil Centre, The University of Sydney, a joint venture with Cancer Council New South Wales, Sydney, NSW, Australia
9. School of Medicine & Dentistry, Griffith University, Gold Coast, QLD, Australia
10. Infectious Diseases Data Observatory, Oxford University, UK
11. Northern Territory Centre for Disease Control, Public Health Division, NT Health, Darwin, Australia
12. National Centre for Epidemiology and Population Health, Australian National University, Canberra, Australia
13. Laboratório Nacional da Saúde, Dili, Timor-Leste
14. Department of Statistics, University of Oxford, UK
15. Pandemic Sciences Institute, University of Oxford, UK

$ Corresponding author

* These authors contributed equally

\+ These authors jointly supervised this work

Corresponding author

Dr Paul Arkell

Email: paul.arkell@menzies.edu.au

Supplementary Methods

Sensitivity analysis on the hierarchical catalytic model

We performed a sensitivity analysis of the catalytic model described in the paper to assess the urban effect on the FOI, by including a urban effect γ_v (Model 2).

$$\text{logit}(\lambda_v) = \mu_v = \mu_n + \delta_v + \gamma_v X_v \qquad \text{Equation S1}$$

where X_v is a binary indicator for village type (urban = 1, rural = 0) and γ_v quantifies the fixed effect for urban villages (having taken rural as reference). We assumed γ_v yo be distributed as $\mathcal{N}(0,1)$.

Model 1 and Model 2 performed similarly according to the statistical measurement LOOIC (leave-one-out cross-validation (LOO) information criterion) (2661.9 vs 2661.3). In Model 2, the FOI estimates were generally higher or equal to Model 1 (Figure S1). The estimated urban logit effect (γ_v) of Model 2 was 1.06 (95% CrI: 0.61, 1.56), suggesting no statistically significant difference in dengue FOI between urban and rural villages.

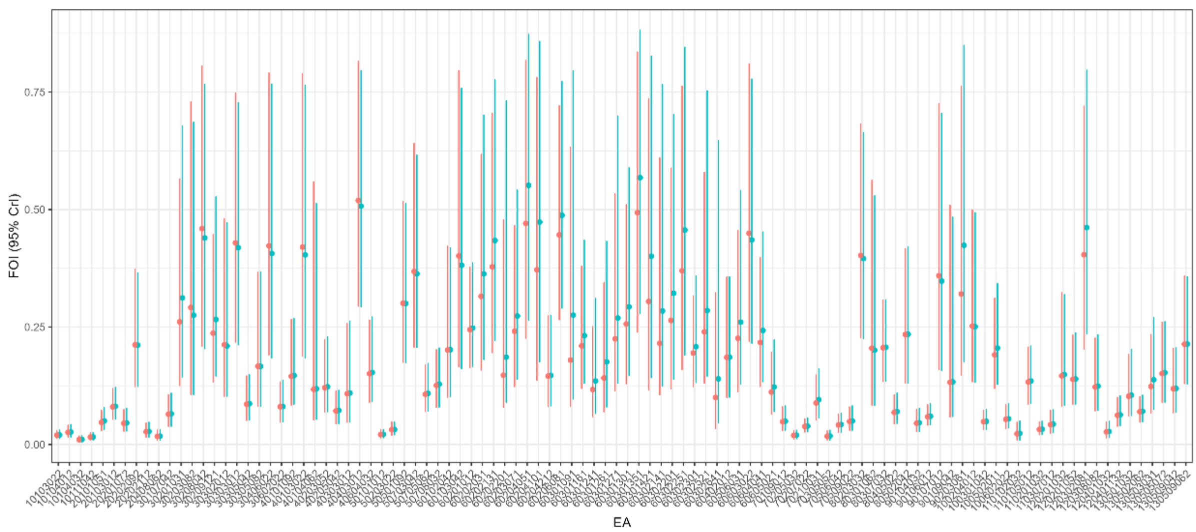

Figure S1. Estimated FOI per EA (λ_v) by Model 1 and 2. Estimated median (point) and 95% CrI (error bar) of the total FOI by EA, coloured by model type (Model 1 in orange and Model 2 in light blue).

Sensitivity analysis at the municipality-level

We performed a sensitivity analysis of the catalytic model described in the paper to assess the variation in the FOI at a lower spatial resolution (municipality-level). The FOI estimates ranged from 0.016 (95% CrI: 0.011, 0.023) in Aileu to 0.332 (95% CrI: 0.277, 0.400) in Dili.

Table S1 Municipality-level FOI estimates. The table reports the median and 95% CrI of the municipality-level FOI.

Municipality	*median*	*ciL*	*ciU*
Aileu	0.016	0.011	0.023
Ainaro	0.061	0.046	0.081
Baucau	0.220	0.170	0.285
Bobonaro	0.201	0.152	0.266
Covalima	0.090	0.069	0.116
Dili	0.332	0.277	0.400
Ermera	0.039	0.030	0.050
Lautem	0.218	0.161	0.297
Liquica	0.115	0.083	0.161
Manatuto	0.110	0.080	0.151
Manufahi	0.060	0.042	0.085
Oecusse	0.130	0.098	0.173
Viqueque	0.138	0.104	0.185

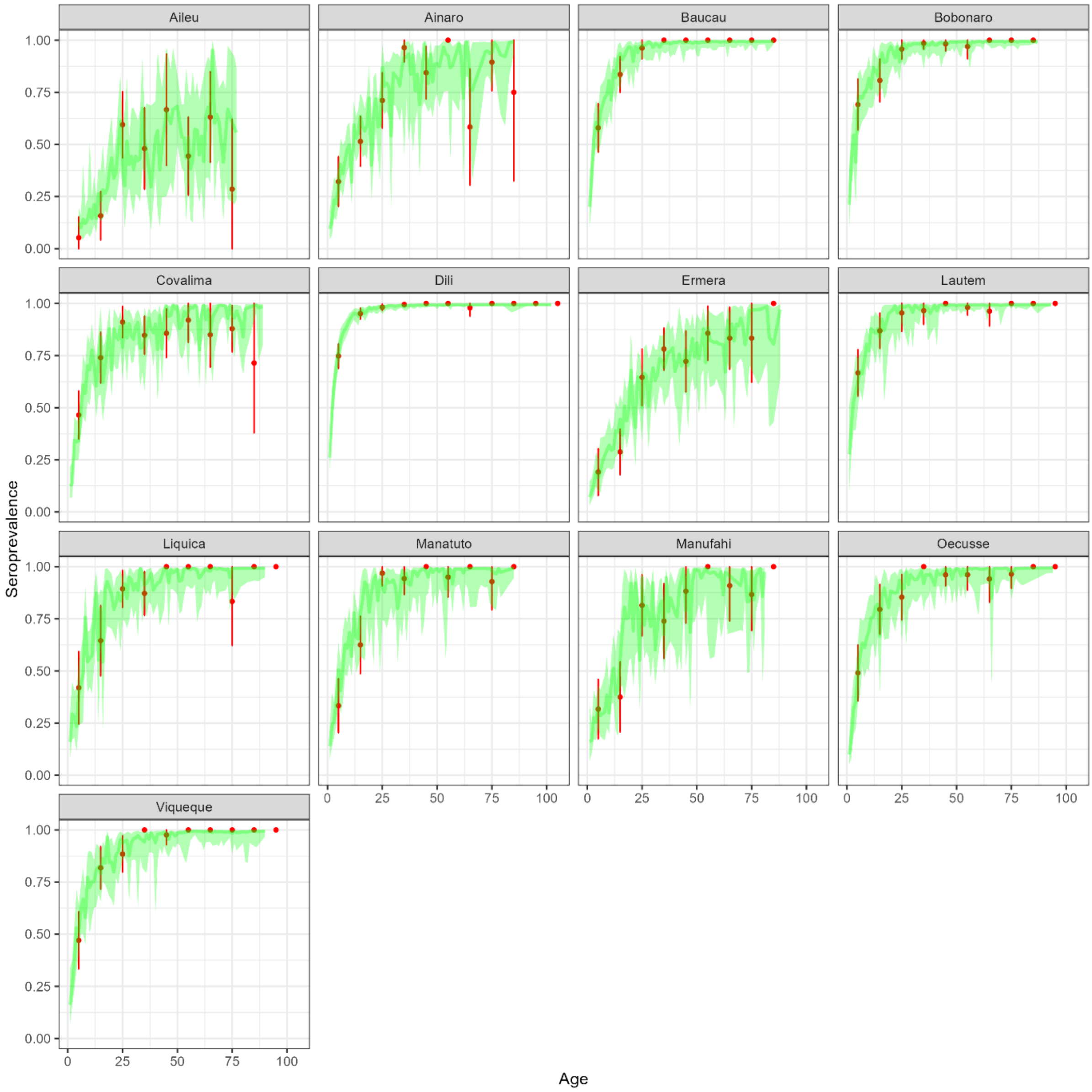

Figure S2. Model fit of the observed seroprevalence data in each municipality in Timor-Leste. The observed seroprevalence is reported in red (points) with the error bars representing the 95% exact binomial confidence interval. Individuals have been grouped into age-groups of 10 years. The estimated seroprevalence is reported in green, with the median shown as a line and the 95% CrI as a shaded area. The x axis represents the age in years, while the y axis represents the seroprevalence.

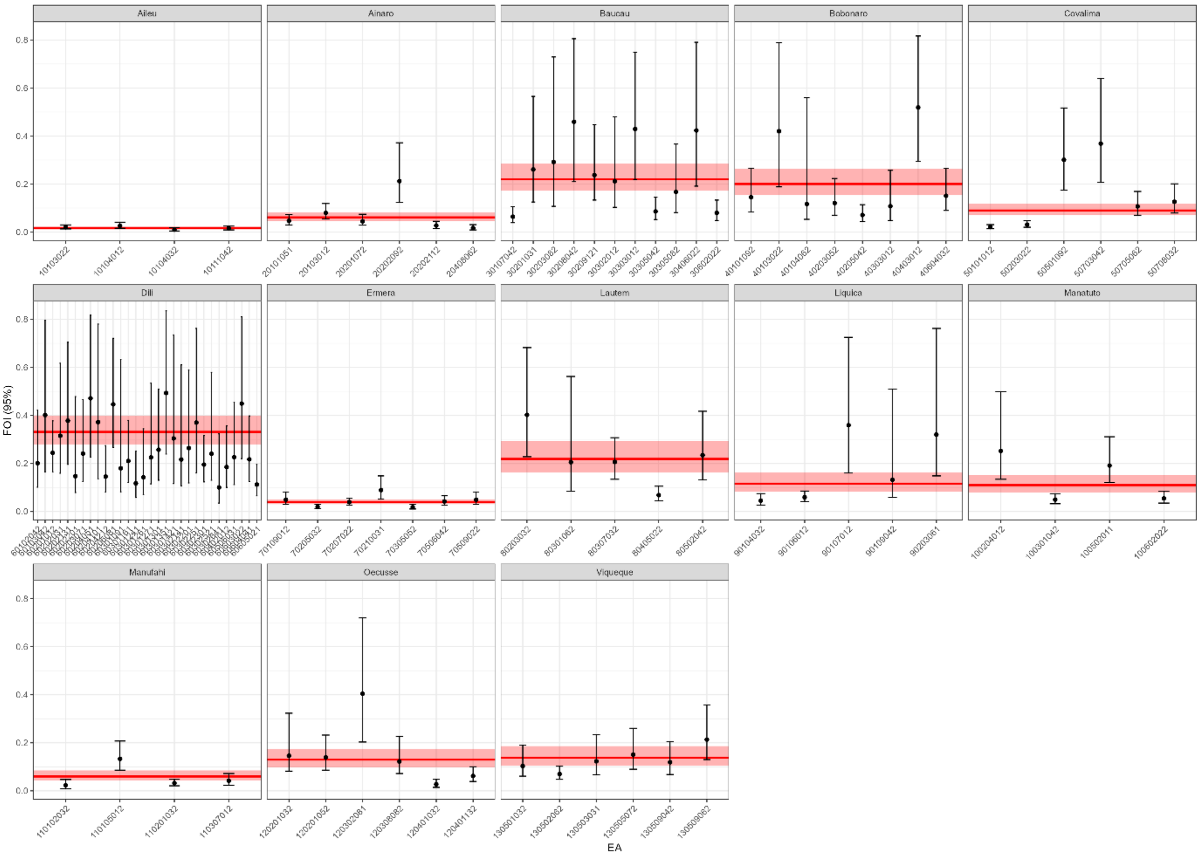

Figure S3. Estimated median (point) and 95% CrI (error bar) of the total FOI by EA and municipality. Each EA-level FOI is plotted as black points (median) with the error bars representing the 95% CrI, the municipality level FOI is plotted as red line (median) and red shaded area (05% CrI). Each box represents one municipality and the EA within.

Sensitivity analysis on borderline IgG results

We performed a sensitivity analysis of the catalytic model described in the paper to assess the impact of removing borderline IgG ELISA results (previously included and considered negative results). In total there were 57 borderline IgG ELISA results. The model was independently fitted with the two datasets (with and without the IgG borderline results). The FOI estimates from the two set of results were similar when the uncertainty around the FOI was smaller, while for those FOI with large uncertainty excluding IgG borderline results increases slightly the median FOI estimates.

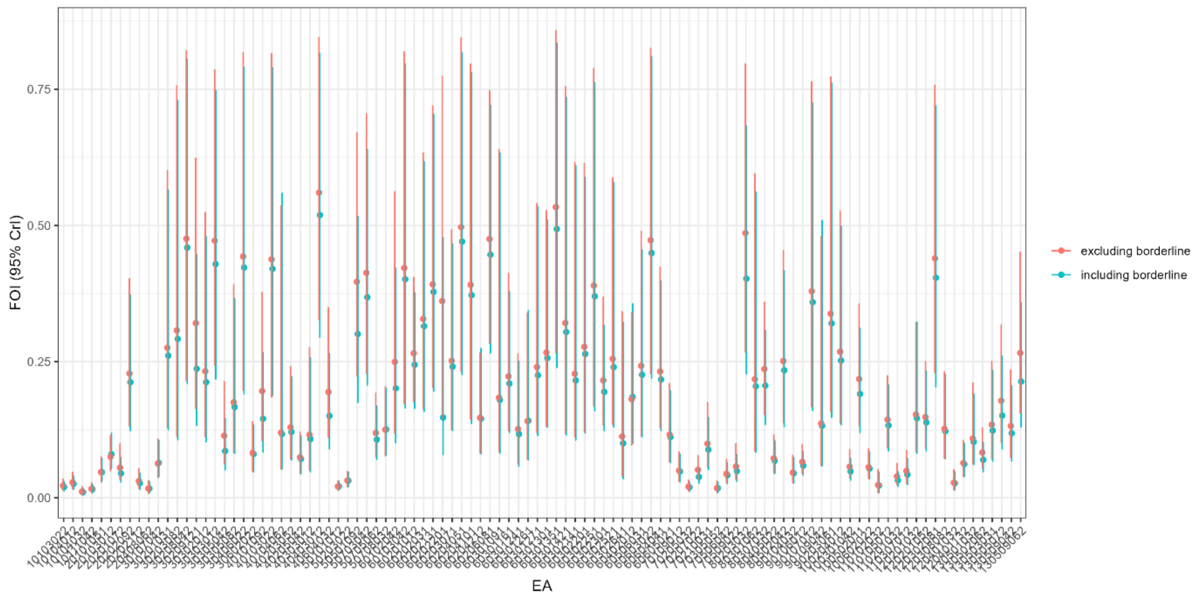

Figure S4. Estimated FOI per EA (λ_v) excluding borderline results. Estimated median (point) and 95% CrI (error bar) of the total FOI by EA, coloured by model type (excluding borderline results in orange and including them in light blue).

Meteorological data

Monthly mean maximum temperature (degrees Celsius), mean minimum temperature (degrees Celsius), cumulative precipitation (mm), and mean vapor pressure (kPa) between January 2011 to December 2022 were extracted from TerraClimate as 5kmresolution [1], [2]. Relative humidity, RH, was calculated from the air temperature, T, and air vapour pressure, e_a, following Equation S1 which first calculates the saturation vapour pressure e_s [3]. The RH was calculated at both minimum and maximum temperature. Table S1 describes the resolution and source of the meteorological, population, and environmental data.

$$e_s = 0.611 e^{\frac{17.27 * T}{237.3 + T}}$$

$$RH = 100 \frac{e_a}{e_s}$$

Equation S1

Spatial random fields

Spatial regression models were fitted to the posterior distributions of the 102 EA-level FOI estimated from the sero-catalytic model, using the stochastic partial differential equations (SPDE) approach in *R-INLA* [6]–[8]. The dengue FOI was assumed to be a spatially-correlated continuous process (a Gaussian field with a Matérn covariance function) which can be represented as a discrete process (Gaussian Markov Random Field, μ, herein called field).

To support the assumption of spatial correlation we assigned each EA its nearest six neighbours, based on distance between the centroid coordinates, and computed the Moran I statistic for the DENV FOI at the coordinates using the *spdep* R package [9]; which indicates presence of spatial autocorrelation when the values are positive with significant p-values (Moran I statistic = 0.27. p-value = 1.585e-08).

The field is built on a triangulated mesh covering the coordinates of the EA centroids. The field is combined with an intercept (α) to model the log-transformed median FOI (λ) per enumeration area l as shown in equation S2:

$$\log(\lambda_l) = \alpha + \mu_l$$

Equation S2

The field μ is the stationary solution to the SPDE which specifies the spatial correlation between two locations i and j, and is characterised by the Matérn covariance function which specifies the distance δ at which i and j are spatially independent and includes a smoothing parameter v and a scaling parameter κ. Following Lindgren *et al.*, 2011, for all values of v, δ can be represented empirically by $\delta = \sqrt{\frac{8v}{\kappa}}$. [10]

We set penalised complexity prior distributions (pc-priors) on the Matérn function hyperparameters (using the *inla.spde2.pcmatern* function) which allow one to describe the prior distribution using probability statements (P) [11]. The prior distribution on δ was set as P(0.001, 0.1) which specifies that there is a probability smaller than 10% that the spatial range is less than 0.001 degrees (which is the approximate minimum distance between any two EA centroid coordinates). The prior distribution on v was set as P(1, 0.10) which states that there is a probability smaller than 10% that the standard deviation of the spatial range is greater than one.

Several meshes were built and a spatial model was fitted to the median estimated FOI using each mesh. The models were compared visually and using the Watanabe-Akaike Information Criterion (WAIC) scores of the spatial models fitted to the data using each mesh (WAIC is a measure of predictive error where a lower score demonstrates a better model fit). For each mesh (Table S2, Figure S5), we specified the minimum angle of the triangles, the offset (which defines the extension of the inner and outer domain), and the maximum edge length of the triangles for the inner and outer domain. We specified meshes A-F using a default boundary around the centroid coordinates of the sampled EAs. We observed that a minimum angle of 25 degrees in mesh A gives medium-sized triangles compared to B and C, which are too small and large respectively, and that increasing the offset in E and F generates a better mesh than in A-D which have singular and irregular triangles in the outer domain (Figure S5). In meshes A-F the boundary extends far into the ocean, so for mesh G and H the boundary was specified using the coordinates of the country outline, to separate the field for Atauro island and Oecusse which are non-continuous with the main island. For mesh H, the cut-off distance was set to 0.02 to build smaller triangles at the boundary edge than for mesh H. The WAIC scores of mesh G and H were 269.72 and

269.44 respectively, so mesh H was used as the preferred mesh in the rest of the analysis.

Supplementary Tables

Table S2: Prior distribution of estimated parameters used in catalytic models.

Parameter	*Description*	*Prior*
δ_v	village-level deviation from the national FOI	$\mathcal{N}(0, \sigma_v)$
δ_h	Household-level deviation from the village FOI	$\mathcal{N}(0, \sigma_h)$
σ_v	Single SD of the village-level deviation from the national FOI	Half-Normal(0.1, 0.1)
σ_h	Single SD of the household-level deviation from the village FOI	Half-Normal(0.1, 0.1)
se	Test sensitivity ($0 < se < 1$)	$\mathcal{N}(0.77, 0.1)$
sp	Test specificity ($0 < sp < 1$)	$\mathcal{N}(0.93, 0.1)$

Table S3. Enumeration area (EA)-, household- and individual- participation rates in each municipality

	Participating EAs	Non-participating EAs	EA participation rate	Participating households	Non-participating households	Household participation rate	Participants	Non-participating household occupants	Individual participation rate
Aileu	4	2	**66.7%**	67	48	58.3%	184	153	54.6%
Ainaro	6	0	**100.0%**	101	39	72.1%	286	145	66.4%
Baucau	11	0	**100.0%**	220	34	86.6%	451	356	55.9%
Bobonaro	8	0	**100.0%**	139	46	75.1%	388	121	76.2%
Covalima	6	0	**100.0%**	124	14	89.9%	356	205	63.5%
Dili	30	0	**100.0%**	437	233	65.2%	1205	1471	45.0%
Ermera	7	5	**58.3%**	115	165	41.1%	329	235	58.3%
Lautem	5	1	**83.3%**	104	37	73.8%	325	184	63.9%
Liquica	5	1	**83.3%**	80	82	49.4%	226	190	54.3%
Manatuto	4	0	**100.0%**	85	11	88.5%	246	75	76.6%
Manufahi	4	1	**80.0%**	56	58	49.1%	178	103	63.3%
Oecusse	6	0	**100.0%**	128	26	83.1%	302	220	57.9%
Viqueque	6	1	**85.7%**	99	65	60.4%	304	189	61.7%
Grand Total	**102**	**11**	**90.3%**	**1755**	858	67.2%	**4780**	**3647**	56.7%

Table S4: Demographic details of participants in each municipality

	Male	% Male	Female	% Female	Median age	Minimum age	Maximum age	Age quartile 1	Age quartile 3	Child	% Child	Adult	% Adult	Rural household	% Rural household	Urban household	% Urban household	Dengue IgG negative	% Dengue IgG negative	Dengue IgG positive	% Dengue IgG positive
Aileu	73	39.7%	111	60.3%	28	5	77	17	52	38	20.7%	146	79.3%	184	100.0%	0	0.0%	109	59.2%	75	40.8%
Ainaro	122	42.7%	164	57.3%	23	1	85	11	43	104	36.4%	182	63.6%	239	83.6%	47	16.4%	100	35.0%	186	65.0%
Baucau	172	38.1%	279	61.9%	32	1	85	16	51	111	24.6%	340	75.4%	360	79.8%	91	20.2%	43	9.5%	408	90.5%
Bobonaro	161	41.5%	227	58.5%	31	1	87	15	46	98	25.3%	290	74.7%	388	100.0%	0	0.0%	34	8.8%	354	91.2%
Covalima	137	38.5%	219	61.5%	30	1	89	12	49	109	30.6%	247	69.4%	356	100.0%	0	0.0%	81	22.8%	275	77.2%
Dili	482	40.0%	723	60.0%	23	1	102	12	38	367	30.5%	838	69.5%	307	25.5%	898	74.5%	72	6.0%	1133	94.0%
Ermera	147	44.7%	182	55.3%	30	1	88	15	46.25	87	26.4%	242	73.6%	295	89.7%	34	10.3%	136	41.3%	193	58.7%
Lautem	135	41.5%	190	58.5%	34	1	93	11	53	121	37.2%	204	62.8%	325	100.0%	0	0.0%	35	10.8%	290	89.2%
Liquica	90	39.8%	136	60.2%	30	1	90	15	51	57	25.2%	169	74.8%	183	81.0%	43	19.0%	41	18.1%	185	81.9%
Manatuto	95	38.6%	151	61.4%	27	1	85	11	46	88	35.8%	158	64.2%	169	68.7%	77	31.3%	57	23.2%	189	76.8%
Manufahi	69	38.8%	109	61.2%	26	1	81	10	45.25	65	36.5%	113	63.5%	178	100.0%	0	0.0%	64	36.0%	114	64.0%
Oecusse	137	45.4%	165	54.6%	32	1	94	14	49	80	26.5%	222	73.5%	240	79.5%	62	20.5%	47	15.6%	255	84.4%
Viqueque	126	41.4%	178	58.6%	29	2	90	14.25	47.75	84	27.6%	220	72.4%	275	90.5%	29	9.5%	44	14.5%	260	85.5%
Grand Total	**1946**	**40.7%**	**2834**	**59.3%**	**28**	**1**	**102**	**13**	**46**	**1409**	**29.5%**	**3371**	**70.5%**	**3499**	**73.2%**	**1281**	**26.8%**	**863**	**18.1%**	**3917**	**81.9%**

Table S5: Force of infection (FOI) estimates by enumeration area (EA) from the sero-catalytic model. Longitude and latitude of each EA centroid is also shown.

EA name	*FOI (95% CrI)*	**Mun-icipality**	***Sub-municipality***	**Suco**	**L*ongitude***	**L*atitude***
10103022	0.020 (0.013, 0.030)	Aileu	Aileu Vila	Fahiria	125.5911	-8.72665
10104012	0.026 (0.016, 0.041)	Aileu	Aileu Vila	Fatubossa	125.5638	-8.81222
10104032	0.010 (0.005, 0.018)	Aileu	Aileu Vila	Fatubossa	125.5421	-8.82593
10111042	0.016 (0.009, 0.025)	Aileu	Aileu Vila	Suco Liurai	125.5216	-8.76602
20101051	0.047 (0.030, 0.073)	Ainaro	Ainaro	Ainaro	125.4992	-8.98757
20103012	0.080 (0.054, 0.119)	Ainaro	Ainaro	Manutaci	125.5197	-8.98526
20201072	0.045 (0.029, 0.074)	Ainaro	Hato-Udo	Foho-Ai-Lico	125.6615	-9.14524
20202092	0.212 (0.124, 0.372)	Ainaro	Hato-Udo	Leolima	125.5784	-9.13306
20202112	0.027 (0.015, 0.045)	Ainaro	Hato-Udo	Leolima	125.5422	-9.19143
20408062	0.017 (0.009, 0.031)	Ainaro	Maubisse	Maubisse	125.5823	-8.83708
30107042	0.064 (0.039, 0.106)	Baucau	Baguia	Lavateri	126.6726	-8.56643
30201031	0.261 (0.125, 0.565)	Baucau	Baucau	Bahu	126.4522	-8.4561
30203082	0.292 (0.107, 0.729)	Baucau	Baucau	Buibau	126.4641	-8.51051
30208042	0.459 (0.210, 0.805)	Baucau	Baucau	SeiÃ§al	126.5248	-8.51821
30209121	0.237 (0.133, 0.447)	Baucau	Baucau	Tirilolo	126.4623	-8.46649
30302012	0.212 (0.103, 0.480)	Baucau	Laga	Libagua	126.6561	-8.4927
30303012	0.429 (0.218, 0.748)	Baucau	Laga	Nunira	126.6294	-8.46225
30305042	0.086 (0.052, 0.146)	Baucau	Laga	Sagadate	126.6853	-8.53214
30305082	0.167 (0.081, 0.366)	Baucau	Laga	Sagadate	126.7171	-8.51676
30406022	0.423 (0.191, 0.790)	Baucau	Quelicai	GuruÃ§Ã	126.6083	-8.57476
30602022	0.080 (0.048, 0.133)	Baucau	Venilale	Baha Mori	126.4297	-8.60586
40101092	0.145 (0.084, 0.266)	Bobonaro	Atabae	Aidabaleten	125.0995	-8.85126
40103022	0.420 (0.188, 0.789)	Bobonaro	Atabae	Hataz	125.164	-8.87183
40104062	0.117 (0.053, 0.559)	Bobonaro	Atabae	Rairobo	125.1716	-8.80121
40203052	0.121 (0.070, 0.223)	Bobonaro	Balibo	Cowa	125.0106	-8.99911
40205042	0.071 (0.044, 0.114)	Bobonaro	Balibo	Leolima	125.0644	-8.90637

40303012	0.108 (0.048, 0.257)	Bobonaro	Bobonaro	Bobonaro	125.3485	-9.04467
40403012	0.519 (0.295, 0.816)	Bobonaro	Cailaco	Goulolo	125.2778	-8.92728
40604032	0.151 (0.090, 0.265)	Bobonaro	Maliana	Raifun	125.208	-8.97344
50101012	0.021 (0.014, 0.031)	Covalima	Fatululic	Fatululic	125.1161	-9.20652
50203022	0.031 (0.02, 0.047)	Covalima	Fatumean	Nanu	125.0136	-9.28893
50501092	0.301 (0.175, 0.517)	Covalima	Suai	Beco	125.3901	-9.19959
50703042	0.368 (0.207, 0.640)	Covalima	Zumalai	Lour	125.3892	-9.07868
50705062	0.107 (0.070, 0.169)	Covalima	Zumalai	Raimea	125.512	-9.16869
50708032	0.126 (0.079, 0.201)	Covalima	Zumalai	Zulo	125.46	-9.15913
60102042	0.201 (0.101, 0.422)	Dili	Atauro	Biqueli	125.6022	-8.16681
60103042	0.401 (0.165, 0.796)	Dili	Atauro	Macadade	125.5427	-8.28541
60201012	0.244 (0.164, 0.377)	Dili	Cristo Rei	Balibar	125.5865	-8.59254
60202031	0.315 (0.159, 0.617)	Dili	Cristo Rei	Becora	125.6024	-8.55976
60202131	0.378 (0.196, 0.704)	Dili	Cristo Rei	Becora	125.5984	-8.56315
60202201	0.147 (0.079, 0.478)	Dili	Cristo Rei	Becora	125.6128	-8.56887
60203071	0.241 (0.124, 0.466)	Dili	Cristo Rei	Bidau Santana	125.5962	-8.55217
60204051	0.471 (0.226, 0.817)	Dili	Cristo Rei	Camea	125.6253	-8.56696
60204101	0.372 (0.136, 0.780)	Dili	Cristo Rei	Camea	125.614	-8.56376
60204212	0.145 (0.081, 0.274)	Dili	Cristo Rei	Camea	125.6383	-8.57996
60206081	0.446 (0.266, 0.721)	Dili	Cristo Rei	Hera	125.6566	-8.53594
60301091	0.180 (0.082, 0.633)	Dili	Dom Aleixo	Bairro Pite	125.5602	-8.55958
60301161	0.210 (0.120, 0.379)	Dili	Dom Aleixo	Bairro Pite	125.5541	-8.56136
60301241	0.117 (0.058, 0.251)	Dili	Dom Aleixo	Bairro Pite	125.5624	-8.56192
60301261	0.142 (0.070, 0.344)	Dili	Dom Aleixo	Bairro Pite	125.5633	-8.56225
60301271	0.225 (0.115, 0.534)	Dili	Dom Aleixo	Bairro Pite	125.5647	-8.56278
60301301	0.257 (0.130, 0.510)	Dili	Dom Aleixo	Bairro Pite	125.5618	-8.56286
60301351	0.493 (0.239, 0.835)	Dili	Dom Aleixo	Bairro Pite	125.5559	-8.57114
60301421	0.304 (0.116, 0.735)	Dili	Dom Aleixo	Bairro Pite	125.5358	-8.58389
60302141	0.216 (0.106, 0.610)	Dili	Dom Aleixo	Comoro	125.5174	-8.54946

60302201	0.264 (0.119, 0.588)	Dili	Dom Aleixo	Comoro	125.5114	-8.56717
60302251	0.370 (0.160, 0.762)	Dili	Dom Aleixo	Comoro	125.5335	-8.54968
60302301	0.195 (0.123, 0.316)	Dili	Dom Aleixo	Comoro	125.534	-8.55257
60302521	0.240 (0.130, 0.579)	Dili	Dom Aleixo	Comoro	125.5309	-8.55841
60302641	0.100 (0.035, 0.323)	Dili	Dom Aleixo	Comoro	125.5356	-8.56578
60402012	0.185 (0.100, 0.356)	Dili	Metinaro	Sabuli	125.7285	-8.53157
60506031	0.226 (0.112, 0.455)	Dili	Nain Feto	Santa Cruz	125.5816	-8.55988
60603022	0.449 (0.220, 0.810)	Dili	Vera Cruz	Dare	125.5549	-8.58741
60604041	0.217 (0.124, 0.398)	Dili	Vera Cruz	Lahane Ocidental	125.5783	-8.57894
60605021	0.112 (0.065, 0.196)	Dili	Vera Cruz	Mascarenhas	125.5799	-8.56463
70109012	0.049 (0.030, 0.080)	Ermera	Atsabe	Malabe	125.3874	-8.92122
70205032	0.019 (0.012, 0.030)	Ermera	Ermera	Mertuto	125.3971	-8.76521
70207022	0.039 (0.027, 0.055)	Ermera	Ermera	Ponilala	125.3753	-8.71904
70210031	0.089 (0.052, 0.148)	Ermera	Ermera	Talimoro	125.4339	-8.72779
70305052	0.018 (0.010, 0.030)	Ermera	Hatulia	Fatubolo	125.372	-8.75788
70506042	0.042 (0.026, 0.065)	Ermera	Railaco	Railaco Leten	125.507	-8.69794
70509022	0.049 (0.030, 0.080)	Ermera	Railaco	Tocoluli	125.4202	-8.71017
80203032	0.402 (0.228, 0.682)	Lautem	LautÃm	Daudere	126.826	-8.46209
80301062	0.205 (0.084, 0.562)	Lautem	Lospalos	Bauro	127.0091	-8.42621
80307032	0.206 (0.134, 0.307)	Lautem	Lospalos	Lore 2	126.9917	-8.55239
80405022	0.068 (0.044, 0.105)	Lautem	Luro	Luro	126.8418	-8.55867
80502042	0.234 (0.131, 0.417)	Lautem	Tutuala	Tutuala	127.2432	-8.44354
90104032	0.045 (0.027, 0.074)	Liquica	Bazartete	Leorema	125.3831	-8.6597
90106012	0.059 (0.041, 0.085)	Liquica	Bazartete	Metagou	125.3671	-8.64346
90107012	0.359 (0.160, 0.725)	Liquica	Bazartete	Motaulun	125.4131	-8.57641
90109042	0.132 (0.059, 0.509)	Liquica	Bazartete	Ulmera	125.4556	-8.58413
90203061	0.320 (0.148, 0.762)	Liquica	LiquiÃÃ¡	Dato	125.3358	-8.59753
100204012	0.252 (0.134, 0.499)	Manatuto	Laclo	Uma Naruc	125.9054	-8.55879
100301042	0.049 (0.032, 0.073)	Manatuto	Laclubar	Batara	125.9519	-8.70867

100502011	0.191 (0.120, 0.311)	Manatuto	Manatuto	Aiteas	126.0385	-8.5159
100602022	0.054 (0.035, 0.084)	Manatuto	Soibada	Leo-Hat	125.967	-8.8575
110102032	0.023 (0.009, 0.047)	Manufahi	Alas	Dotik	125.8308	-8.96764
110105012	0.133 (0.086, 0.207)	Manufahi	Alas	Uma Berloic	125.9276	-9.12137
110201032	0.032 (0.021, 0.048)	Manufahi	Fatuberlio	Bubussuso	125.7666	-8.89974
110307012	0.042 (0.024, 0.072)	Manufahi	Same	Rotuto	125.6011	-8.97127
120201032	0.146 (0.082, 0.323)	Oecusse	Oesilo	Bobometo	124.3554	-9.30304
120201052	0.139 (0.086, 0.232)	Oecusse	Oesilo	Bobometo	124.3792	-9.32518
120302081	0.404 (0.203, 0.720)	Oecusse	Pante Macassar	Costa	124.3427	-9.20812
120308082	0.122 (0.072, 0.226)	Oecusse	Pante Macassar	Taiboco	124.2832	-9.29483
120401032	0.027 (0.014, 0.048)	Oecusse	Passabe	Abani	124.3378	-9.43847
120401132	0.062 (0.039, 0.100)	Oecusse	Passabe	Abani	124.3278	-9.46321
130501032	0.103 (0.061, 0.191)	Viqueque	Viqueque	Bahalarauain	126.2705	-8.91203
130502062	0.070 (0.048, 0.102)	Viqueque	Viqueque	Bibileo	126.3101	-8.93673
130503031	0.123 (0.067, 0.234)	Viqueque	Viqueque	Caraubalo	126.3673	-8.86818
130505072	0.151 (0.090, 0.260)	Viqueque	Viqueque	Luca	126.2574	-8.92059
130509042	0.119 (0.068, 0.205)	Viqueque	Viqueque	Uma Uain Craic	126.3781	-8.87941
130509062	0.213 (0.130, 0.358)	Viqueque	Viqueque	Uma Uain Craic	126.3879	-8.89039

Table S16: Meteorological, environmental, and demographic variables.

Variable	Source	Spatial resolution	Temporal resolution	Number of datapoints
Middle infrared reflectance (MIR)	MODIS	1km	8 days	14057311
Enhanced vegetation index (EVI)	MODIS	1km	8 days	14057311
Precipitation	TerraClimate	5km	1 month	166752
Maximum air temperature at ground level during 24-hour period (Tmax)	TerraClimate	5km	1 month	166752
Minimum air temperature at ground level during 24-hour period (Tmin)	TerraClimate	5km	1 month	166752
Relative humidity at Tmax	TerraClimate	5km	1 month	166752
Relative humidity at Tmin	TerraClimate	5km	1 month	166752
Elevation	Worldclim	1km	NA	25157
Population	Landscan	1 km	1 year	234546

Table S7. Parameters used to build triangulated meshes for the spatial field.

Mesh	Minimum angle (degrees)	Maximum edge length	Offset	Boundary	Coordinates	Cut-off distance	WAIC
A	25	0.2, 0.4	0.2, 0.3	null	EA centroids	0.03	241.52
B	35	0.2, 0.4	0.2, 0.3	null	EA centroids	0.03	218.27
C	15	0.2, 0.4	0.2, 0.3	null	EA centroids	0.03	242.56
D	25	0.5, 0.5	0.2, 0.3	null	EA centroids	0.03	245.36
E	25	0.2, 0.4	0.2, 0.6	null	EA centroids	0.03	241.52
F	25	0.2, 0.4	0.6, 0.6	null	EA centroids	0.03	241.16
G	25	0.2, 0.4	0.2, 0.6	country boundary	null	0.03	269.72
H	25	0.2, 0.4	0.2, 0.6	country boundary	null	0.02	269.44

Supplementary Figures

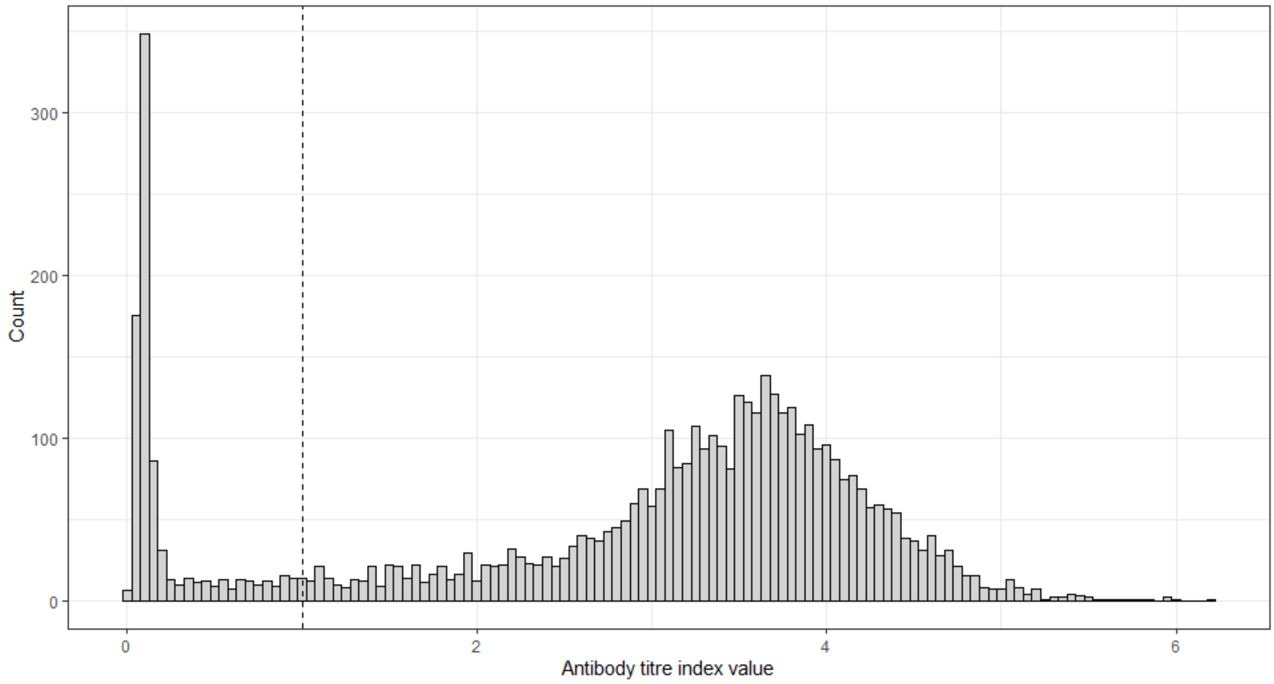

Figure S5. Histogram showing raw IgG antibody titres from the serosurvey. A dashed vertical line is shown to represent the cutoff used to classify the samples as seronegative or seropositive.

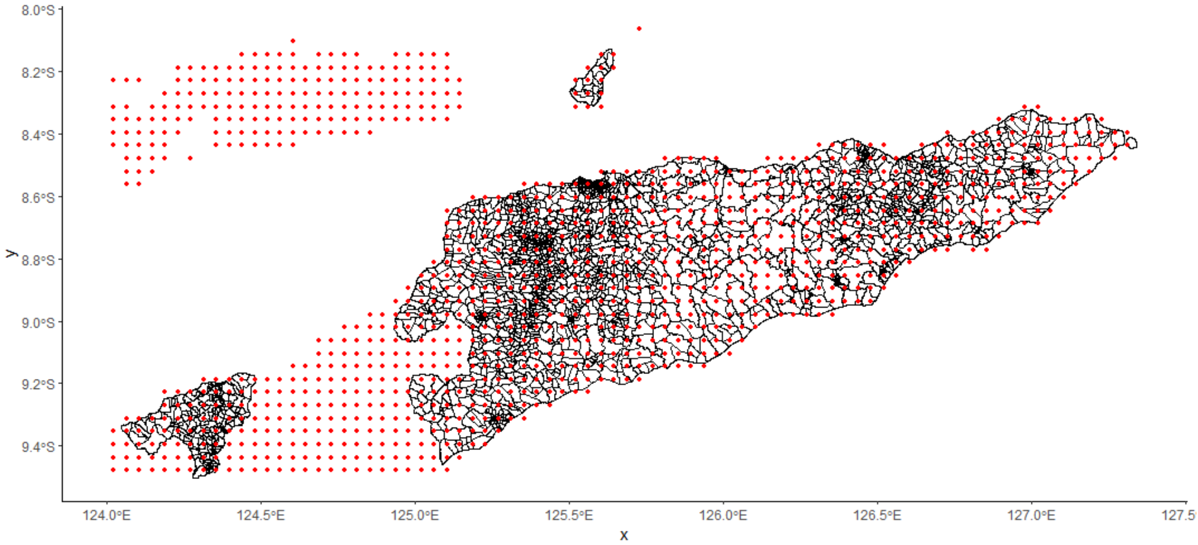

Figure S6: Enumeration areas of Timor-Leste, in black, overlaid with points showing the centroids of the 5km-resolution meteorological data, in red.

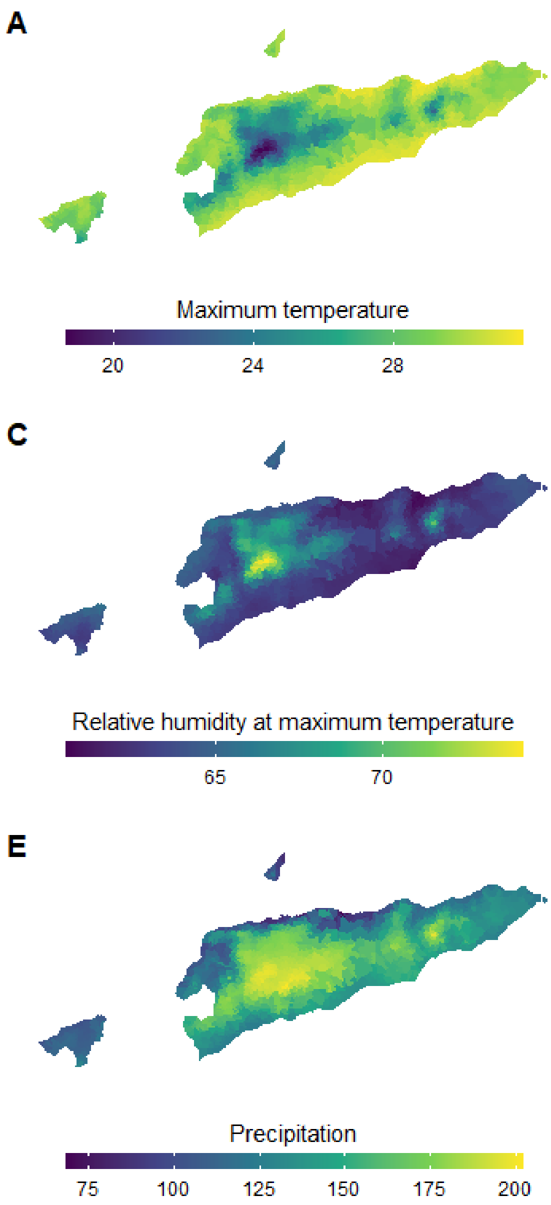

Figure S7: Maps of the average (A) maximum temperature, (B) minimum temperature, (C) relative humidity at minimum temperature, (D) relative humidity at maximum temperature, and (E) precipitation for each enumeration area in Timor-Leste.

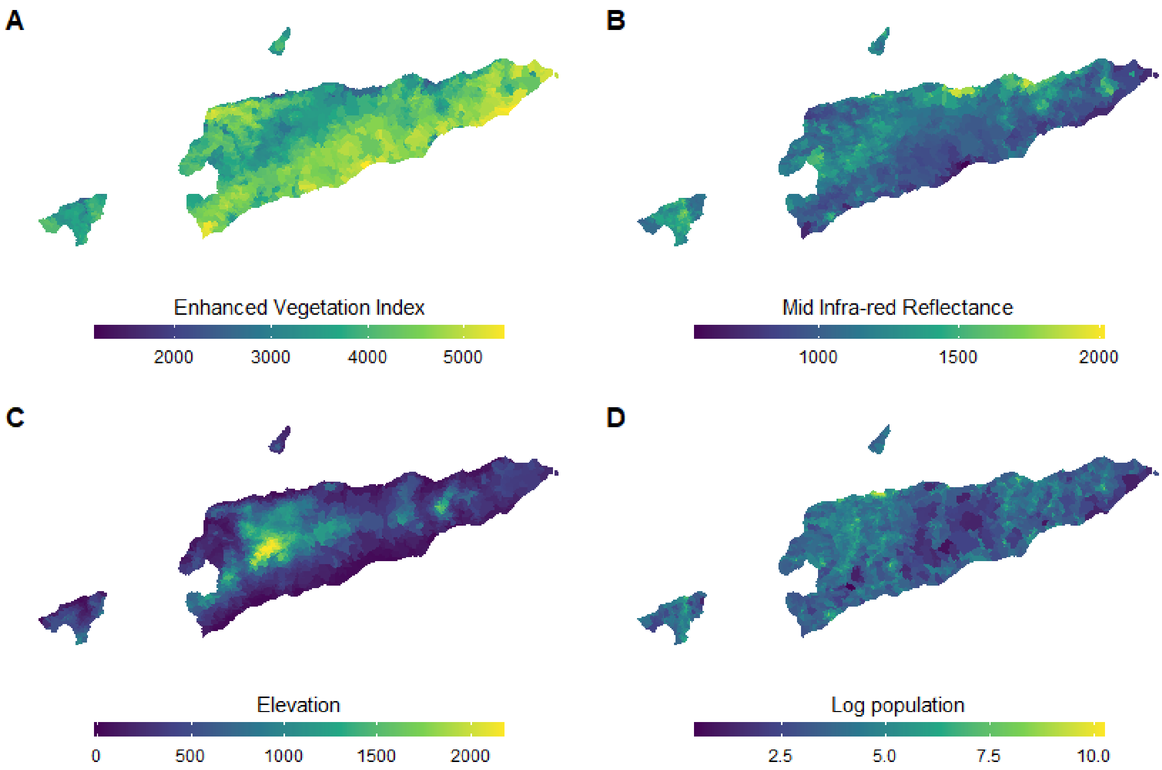

Figure S8: Maps of the average (A) Enhanced Vegetation Index (EVI), (B) Mid infra-red reflectance (MIR), (C) elevation above sea level, and (D) population on the log scale for each enumeration area in Timor-Leste.

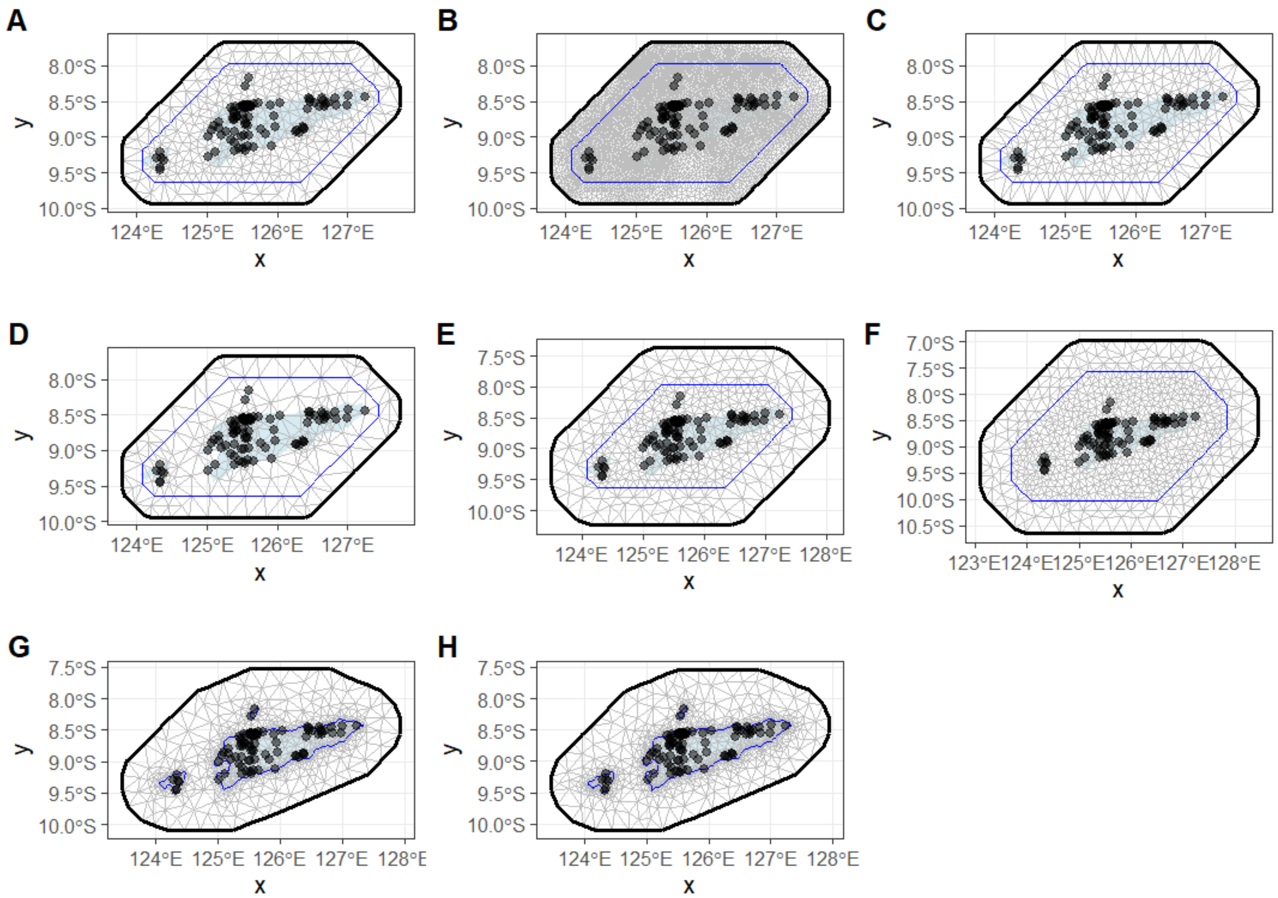

Figure S9: Triangulated meshes tested in the analysis, with Timor-Leste shown in light blue, the coordinates of the centroids of the sampled enumeration areas represented as black points, and boundaries in dark blue.

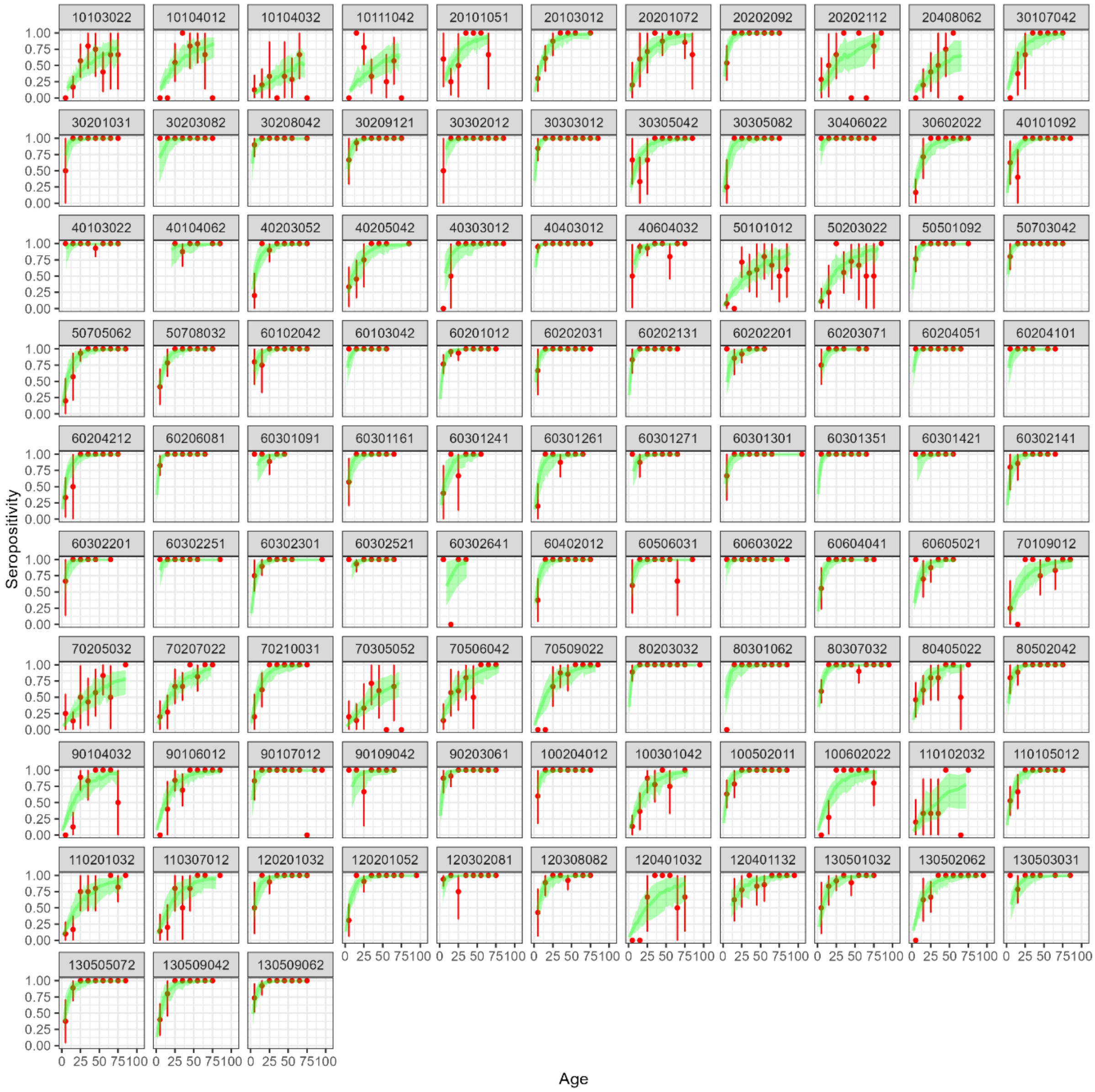

Figure S10. Model fit of the observed seroprevalence data in each EA in Timor-Leste. The observed seroprevalence is reported in red (points) with the error bars representing the 95% exact binomial confidence interval. Individuals have been grouped into age-groups of 10 years. The estimated seroprevalence is reported in green, with the median shown as a line and the 95% CrI as a shaded area. The x axis represents the age in years, while the y axis represents the seroprevalence. Each panel represents a different EA identified by the number in the title.

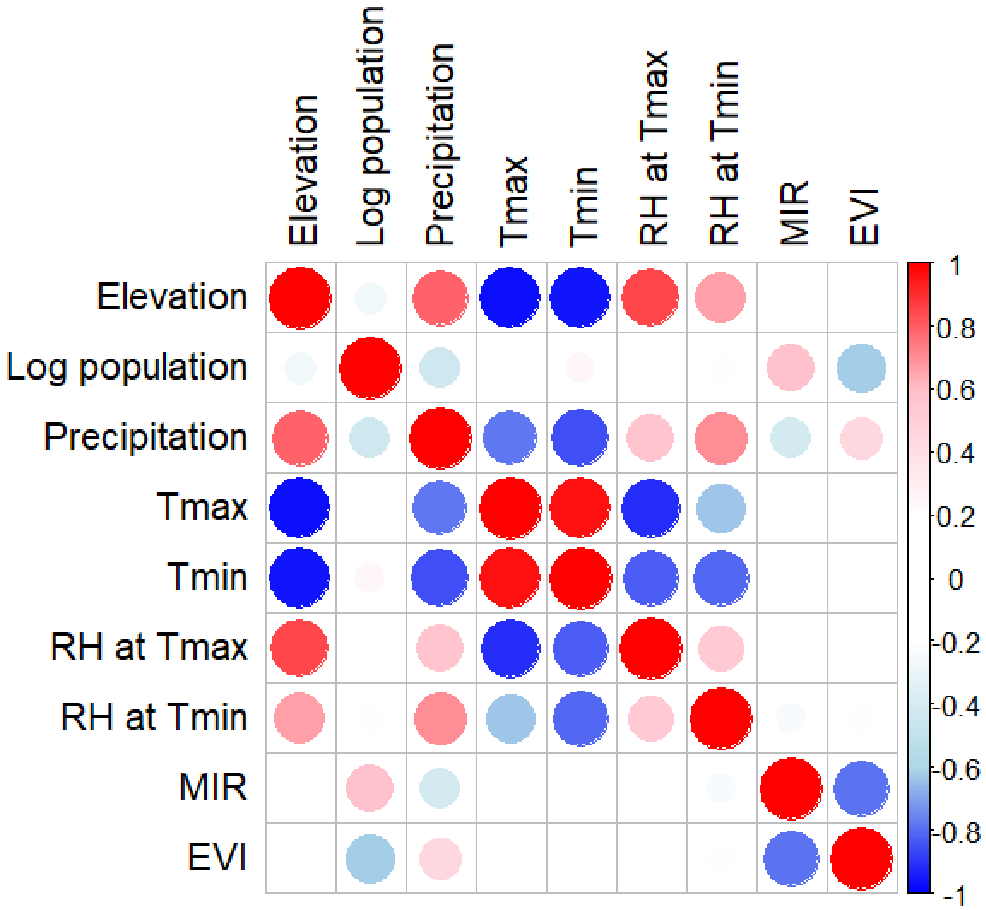

Figure S11: Collinearity of the meteorological and demographic variables. The points are scaled and coloured with their Pearson's correlation coefficient.

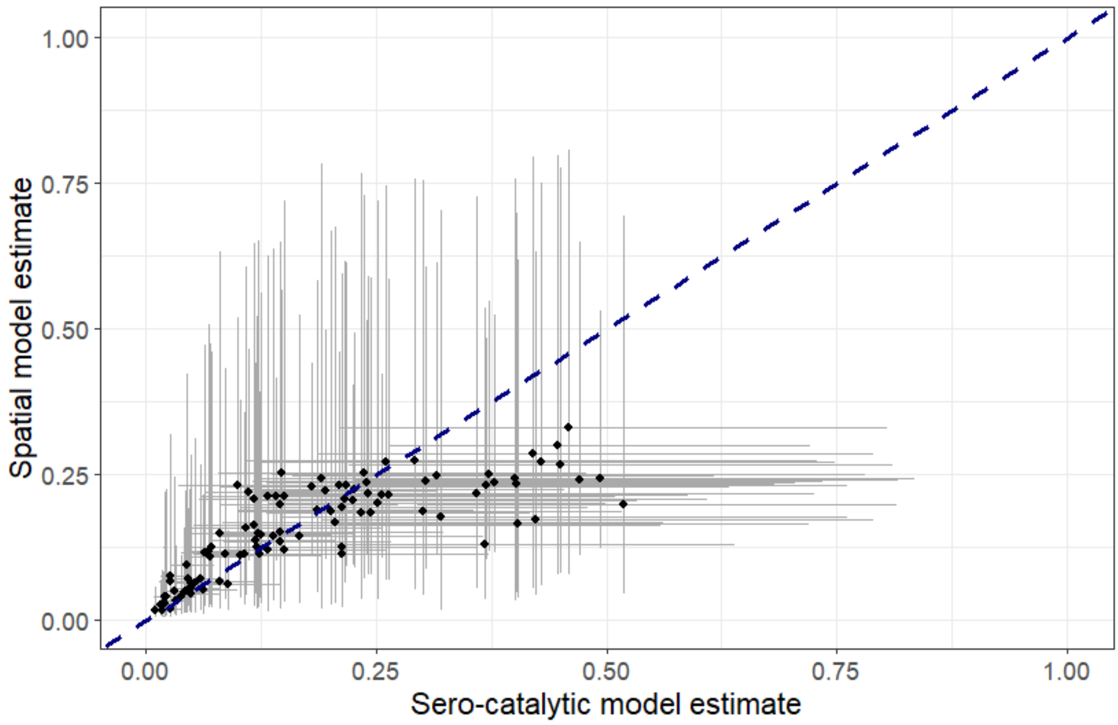

Figure S12: Cross-validation of the spatial model. Median and 95% credible intervals of the ensemble spatial model dengue FOI estimates on the y-axis, compared to the median and 95% CrI of the sero-catalytic model dengue FOI estimates on the x-axis, for the 102 sampled enumeration areas.

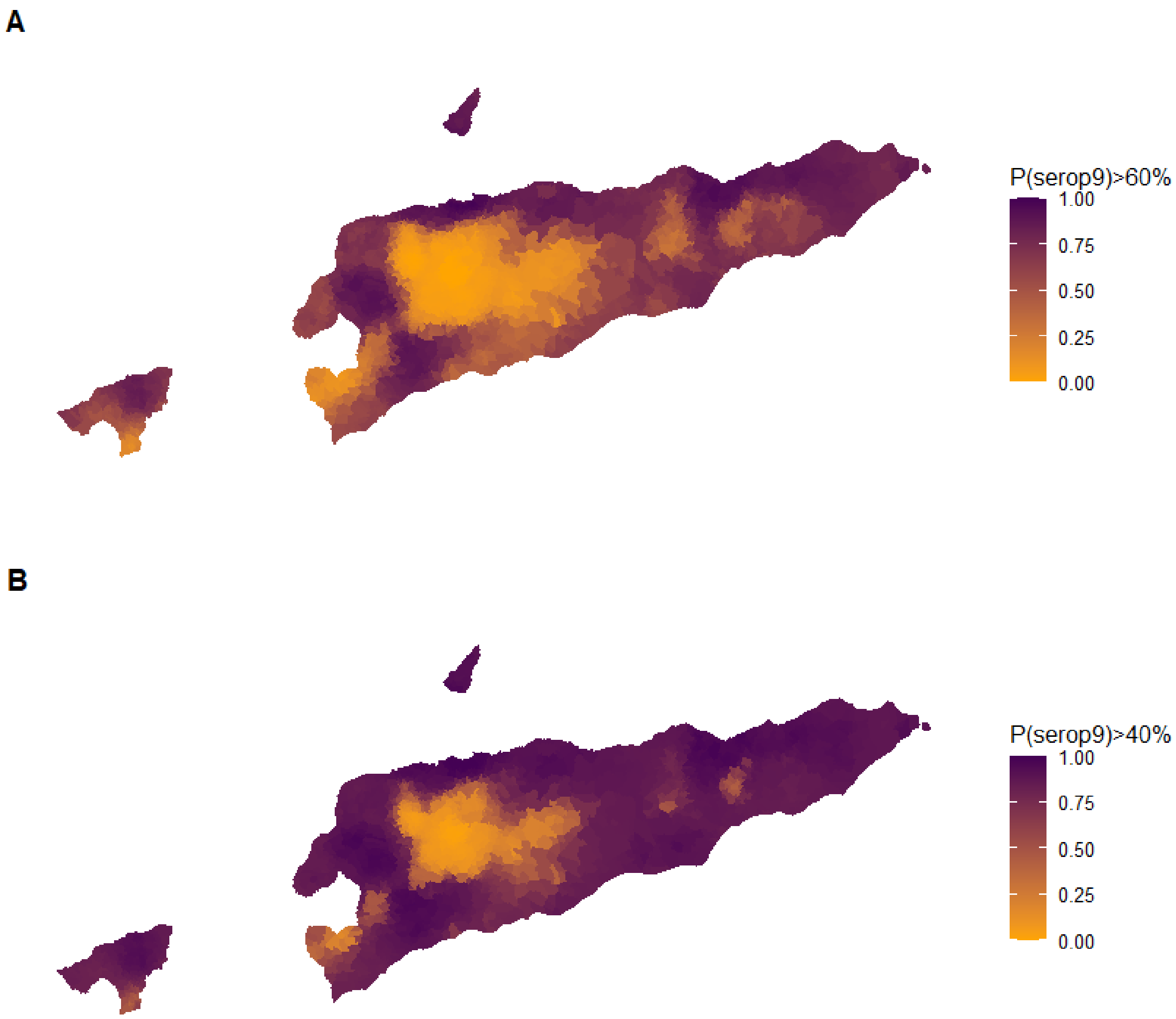

Figure S13: Exceedance probability maps for the predicted seroprevalence at 9 years of age (serop9) across Timor-Leste. The probability that the serop9 exceeds 60% (A) and 40% (B) are shown, and are extracted from the joint spatial model estimated posterior distributions.

Supplementary References

[1] "TerraClimate." [Online]. Available: https://www.climatologylab.org/terraclimate.html.

[2] J. T. Abatzoglou, S. Z. Dobrowski, S. A. Parks, and K. C. Hegewisch, "TerraClimate, a high-resolution global dataset of monthly climate and climatic water balance from 1958–2015," *Sci. Data 2018 51*, vol. 5, no. 1, pp. 1–12, Jan. 2018.

[3] Alduchov A Oleg and Eskridge E Robert, "Improved Magnus Form Approximation of Saturation Vapor Pressure," *J. Appl. Meteorol. Climatol.*, 1996. vol. 35, no. 4, pp.601-609

[4] Statistics Department Timor-Leste Ministry of Infrastructure, "EA kml shapefile." 2023.

[5] D. Baston, "exactextractr: Fast Extraction from Raster Datasets using Polygons." 2020.

[6] H. Bakka *et al.*, "Spatial modeling with R-INLA: A review," *Wiley Interdiscip. Rev. Comput. Stat.*, vol. 10, no. 6, pp. 1–33, 2018.

[7] F. Lindgren, H. Rue, and J. Lindström, "An explicit link between Gaussian fields and Gaussian Markov random fields: the stochastic partial differential equation approach," *J. R. Stat. Soc. Ser. B (Statistical Methodol.*, vol. 73, no. 4, pp. 423–498, Sep. 2011.

[8] M. Blangiardo and M. Cameletti, *Spatial and Spatio-temporal Bayesian Models with R-INLA*. John Wiley & Sons Ltd, Chichester, United Kingdom. 2015.

[9] R. Bivand *et al*, "spdep: Spatial Dependence: Weighting Schemes, Statistics". 2023

[10] F. Lindgren and H. Rue, "An explicit link between Gaussian fields and Gaussian Markov random fields: the stochastic partial differential equation approach," *J. R. Stat. Soc. Ser. B*, vol. 73, no. 4, pp. 423–498, 2011.

[11] G. A. Fuglstad, D. Simpson, F. Lindgren, and H. Rue, "Constructing Priors that Penalize the Complexity of Gaussian Random Fields," *https://doi.org/10.1080/01621459.2017.1415907*, vol. 114, no. 525, pp. 445–452, Jan. 2018.